Energy Research and Development Division

FINAL PROJECT REPORT

Improvement of an Airborne Natural Gas Leak-Detection System

California Energy Commission

Edmund G. Brown Jr., Governor

September 2017 | CEC-500-2017-030

PREPARED BY:

Dr. Stephen Conley
Department of Land, Air and Water Resources
Plant and Environmental Sciences 3138
1 Shields Avenue
University of California, Davis
Davis, CA 95616

PREPARED FOR:
California Energy Commission

Guido Franco
Contract/Project Manager

Contract Number: 500-13-005

Aleecia Gutierrez
Office Manager
Energy Generation Research Office

Laurie ten Hope
Deputy Director
ENERGY RESEARCH AND DEVELOPMENT DIVISION

Robert P. Oglesby
Executive Director

ACKNOWLEDGEMENTS

This report was submitted in fulfillment of Agreement No. 500-13-005. The author acknowledges the generous support provided by the California Energy Commission to conduct this research. The author benefited from discussions with technical staff at the California Energy Commission, California Air Resources Board, the National Oceanic and Atmospheric Administration, Pacific Gas & Electric, and others.

PREFACE

The California Energy Commission's Energy Research and Development Division manages the Natural Gas Research and Development program, which supports energy-related research, development, and demonstration not adequately provided by competitive and regulated markets. These natural gas research investments spur innovation in energy efficiency, renewable energy and advanced clean generation, energy-related environmental protection, energy transmission and distribution and transportation.

The Energy Research and Development Division conducts this public interest natural gas-related energy research by partnering with RD&D entities, including individuals, businesses, utilities and public and private research institutions. This program promotes greater natural gas reliability, lower costs and increases safety for Californians and is focused in these areas:

- Buildings End-Use Energy Efficiency.
- Industrial, Agriculture and Water Efficiency
- Renewable Energy and Advanced Generation
- Natural Gas Infrastructure Safety and Integrity.
- Energy-Related Environmental Research
- Natural Gas-Related Transportation.

Improvement of an Airborne Natural Gas Leak-Detection System is the final report under Contract Number 500-13-005, conducted by the University of California, Davis. The information from this project contributes to Energy Research and Development Division's EPIC Program.

All figures and tables are the work of the author(s) for this project unless otherwise cited or credited.

For more information about the Energy Research and Development Division, please visit the Energy Commission's website at www.energy.ca.gov/research/ or contact the Energy Commission at 916-327-1551.

ABSTRACT

Airborne platforms can be used to detect and quantify leaks in the natural gas system (from extraction to delivery), and often provide the only reasonable option when time is of the essence. Through controlled release experiments (methane and ethane), power plant comparisons and the wealth of statistics surrounding the 2015 Aliso Canyon leak, the research team demonstrated ±20% accuracy in measuring emission rates from a variety of sources, typically in less than one hour. For detecting and localizing unknown sources, the research team demonstrated that three passes at the appropriate downwind distance without detection provides a 95 percent confidence there is no leak. Additionally, with steady winds, the predicted leak location was found to be within 200 meters of the actual leak.

Keywords: (leak detection, emissions, airplane, methane, ethane)

Please use the following citation for this report:

Conley, Stephen. 2017. *Improvement of an Airborne Natural Gas Leak-Detection System*. California Energy Commission. Publication Number: CEC-500-2017-030.

TABLE OF CONTENTS

LIST OF FIGURES

Page

LIST OF TABLES

Page

EXECUTIVE SUMMARY

Introduction

Methane is a major greenhouse gas, which is 84 times more potent than carbon dioxide (CO_2) over a 20-year time horizon. Methane is responsible for nine percent of California's total greenhouse gas emissions. An extensive understanding on methane sources, including locations, emission potential, distribution and contribution is essential for California to improve the emission inventory and develop policy programs.

Assembly Bill 1496 (AB 1496) requires the State to monitor and measure high methane emission hotspots within California using the best available scientific and technical methods. This demands new technology and techniques to quickly locate and measure unknown methane sources (e.g. pipelines, wells, storage facilities, etc.). Airplanes offer unprecedented speed and the ability to survey areas inaccessible to ground vehicles (e.g. complex terrain).

Project Purpose

This project evaluated how well the use of a small research aircraft instrumented with methane and ethane analyzers could identify and quantify methane leaks from the natural gas system.

In October 2015, 8,000 residents of Porter Ranch were evacuated during the Aliso Canyon natural gas leak. The Governor's decision to declare a state of emergency would have been unlikely without information about the magnitude of the leak. Timely knowledge of sources is necessary for the state to appropriately respond to an incident. Additionally, detection of leaks before catastrophic failure can substantially reduce methane emissions and protect life and property.

Project Process

Previous attempts using a small research aircraft were hampered by confusing nearby methane sources (e.g. landfills, dairies, etc.). To isolate oil and natural gas emissions, the Energy Commission provided an ethane analyzer for this project. Two types of flights were conducted during this project: pipeline flights, and source quantification flights (e.g. Aliso Canyon). A new technique was developed and tested for the quantifying airborne methane sources using an aircraft to fly circles around the natural gas source, taking measurements and comparing the surface change to the net change of emissions in the region bounded by the flight path.

Project Results

The ability to quantify sources was significantly improved by this project. The research team had anticipated better results during the pipeline leak detection flights, however non-steady winds complicated the team's ability to localize the leak. With enough passes, leaks could be localized to an acceptable level, yet the multiple passes over the location negated any financial advantage to using this technology over existing techniques (e.g. infrared cameras).

Benefits to California

Methane leaks cost Californians in many ways. Lost revenue and cleanup costs translate into higher utility rates, release of potentially hazardous chemicals into the air can present health issues and finally,

associated fires and explosions can cost lives. Early detection can reduce the dangers ratepayers are exposed and steps can be taken to reduce health and safety impacts.

CHAPTER 1

1.1 Introduction

The accuracy of inventories of greenhouse gas emissions is crucial as initial steps are being made to regulate global emissions. Numerous sources, however, are often highly variable in physical size, magnitude, and duration that rigorous verification is challenging. Nevertheless, measurement techniques have markedly improved in the last decade, and are being used in unprecedented numbers to refine emission inventories [*Nisbet and Weiss*, 2010]. Most so called "bottom-up" inventories are developed by aggregating statistical correlates of individual process emissions to such mapping variables as population density, energy consumption, head of cattle, etc. extrapolating from a relatively small number of examples. Atmospheric scientists, however, have long strove to use measurements from global surface networks, aircraft campaigns, and satellites to determine emissions based on the amounts and build-up of observed trace gases. The latter, "top-down" approach conveniently integrates the multitudes of sources, however, is heavily reliant on a skillful knowledge of atmospheric transport. Attempts to reconcile these two distinct methods on global [*Muhle et al.*, 2010] and continental scales [*Gerbig et al.*, 2003; *Miller et al.*, 2013] have often been underestimated by the "bottom-up" methods by a factor 1.5 or more.

The solution to both of these problems was to modify the flight path to include a closed path around the facility. In this way, there are as many upwind measurements as there are downwind, and neighboring sources, provided they can be excluded from the flight path, can be separated from the emissions estimate. This technique relies on Gauss' theorem to equate the flux measurements taken around the closed path to the divergence within, as described in later sections.

The "top-down" measurements can be conducted at all the atmospheric scales to better understand and identify the emissions at comparable scales. For long-lived compounds like greenhouse gases, which readily disperse throughout the atmosphere, the global scale is very instructive. The seminal experiment started with Keeling's infamous CO_2 curve [1960], and has continued through more contemporary techniques by [*Hirsch et al.*, 2006; *Neef et al.*, 2010] for CH_4 and N_2O, respectively. At progressively smaller scales more details of the source strengths and apportionment can be made: from synoptic or continental scales which can help constrain national inventories [*Bergamaschi et al.*, 2005] or specific biogeographic regions [*Gallagher et al.*, 1994], to mesoscale investigations which can make estimates of urban emissions [*Mays et al.*, 2009; *Turnbull et al.*, 2011; *Wecht et al.*, 2014] or oil and gas fields [*Karion et al.*, 2013; *Petron et al.*, 2014] and even down to individual area sources of order 10-100 m [*Denmead et al.*, 1998; *Lavoie et al.*, 2015; *Roscioli et al.*, 2015].

Aircraft measurements are central to many of these "top-down" methods because they see a more fully integrated signal and can cover relatively large volumes of the atmospheric boundary layer where most emissions are concentrated, but deployments tend to be costly and thus sporadic. The aircraft methods used so far tend to be one of three main types. First, there is the eddy covariance technique that is made at low altitudes wherein the vertical fluxes of gases carried by the turbulent wind are measured by tracking rapid fluctuations of both [*Hiller et al.*, 2014; *Ritter et al.*, 1994; *Yuan et al.*, 2015]. This method is generally thought to be the most direct, but it is limited to small footprint regions which must be repeatedly sampled for sufficient statistical confidence, requires a sophisticated vertical wind

measurement, and can be subject to complications by any flux divergence between the surface and the lowest flight altitude.

The second, and by far the most common, approach is what chemists usually refer to as "mass balance" and what is known in the turbulence community as a "scalar budget" technique. Many different sets of assumptions and sampling strategies are employed, but overall an attempt is made to sample the main dispersion routes of the surface emissions as they make their way into the greater atmosphere, first off accumulating in the boundary layer. The scales most tenable by this method are from a few kilometers [*Alfieri and Blanken*, 2012; *Hacker et al.*, 2016; *Hiller et al.*, 2014; *Tratt et al.*, 2014] to tens of kilometers [*Caulton et al.*, 2014; *Karion et al.*, 2013; *Wratt et al.*, 2001] to even potentially hundreds of kilometers [*Beswick et al.*, 1998; *Chang et al.*, 2014], although each scale has its own advantages and difficulties.

The third general method of source quantification is by scaling measurements in the atmosphere to another trace gas with a metered or otherwise known emission rate and assuming that the exact details of the overall mixing patterns for both diffuse out in the average. Typically this tracer release is applied to small scales of 10-100s of meters [*Czepiel et al.*, 1996; *Lamb et al.*, 1995; *Roscioli et al.*, 2015] but has been attempted at the basin scale [*Peischl et al.*, 2013] given ample confidence in regional emission inventories of reference gases like CO_2 or carbon monoxide (CO).

The airborne mass balance flight strategies can be grouped into three basic patterns: a single height transect around a source assuming a completely uniformly mixed boundary layer [*Karion et al.*, 2013; *Turnbull et al.*, 2011]; upwind/downwind [*Wratt et al.*, 2001] or sometimes just downwind flight legs [*S Conley et al.*, 2016; *Hacker et al.*, 2016; *Ryerson et al.*, 1998]; and multiple flight legs at different altitudes, either in a stacked box configuration [*Alfieri et al.*, 2012; *Gordon et al.*, 2015; *Kalthoff et al.*, 2002]; or just a 'screen' on the downwind face of the box [*Lavoie et al.*, 2015; *Mays et al.*, 2009]. The research group describes a new airborne method borne out of a necessity to identify source emissions to within 100s of m in a large heterogeneous field of potential sources.

The novel technique applies an aircraft flight pattern that limns a virtual cylinder around a source of interest and, using only observed horizontal wind and traces gas concentrations, applies Gauss' theorem to estimate the flux divergence through that cylinder. By integrating the outward horizontal fluxes along each point along the flight path, the effects of upwind sources can be minimized. In practice, an emission estimate can be completed in roughly 30 minutes of flight time. Making an accurate estimate requires selection of an appropriate circling radius based on the micrometeorological conditions inferred in flight by the aircraft. The pattern must be wide enough for the plume to mix sufficiently in the vertical, yet small enough that the plume enhancements stand out sufficiently from the background noise.

This project was aimed at improving techniques to localize and quantify surface sources of trace gases, primarily methane. Prior to this study, aircraft relied on transects upwind and downwind to estimate the flux in and out of a theoretical control volume. This presented several challenges and sources of uncertainty. First, in the interest of time, far more flight time was spent on the downwind side of a source because of the presumption that the upwind region was "background". Unfortunately, that assumption is often complicated by the fact that the region upwind of one source is frequently downwind of another. The second complication is one of attribution; the fact that an enhancement is seen in the general downwind area of a source does not mean it originated from the source. Potential sources are frequently

densely packed and there is enough variability in the wind to easily shift the back trajectory from one source to a neighboring facility.

Regardless of the method selected, flight paths can rarely be designed to capture the entire vertical extent of the atmospheric boundary layer. In most cases, flight restrictions limit the aircraft to above 150 meters, suggesting that for typical boundary layer heights of 1 km, roughly 15% of the boundary layer may be excluded. Depending on the buoyancy of the source and the downwind distance, the bulk of the plume can be contained in this region [*Weil et al.*, 2012]. Making an accurate estimate requires selection of an appropriate circling radius, large enough for the plume to mix sufficiently in the vertical, yet small enough that the plume enhancements stand out sufficiently from the noise.

To the knowledge of the research team, none of these previous studies have benefited from a "known" emission rate experiment to test the strategy as conducted here.

1.2 Instrumentation

The airborne detection system is flown on a fixed wing single engine Mooney aircraft, extensively modified for research as described in [*Conley et al.*, 2014]. Ambient air is collected through tubes protruding from the right wing (Kynar, Teflon and stainless steel). Methane and CO_2 measurements are made with a Picarro 2301f cavity ring down spectrometer as described in [*Crosson*, 2008].

Ethane measurements are made with an Aerodyne Methane/Ethane tunable diode infrared laser direct absorption spectrometer [*Yacovitch et al.*, 2014]. There is an inherent lag in both analyzers, caused primarily by the ~5 meters of tubing. That lag depends on the flow rate, tube diameter and delays inherent in the system. The research team uses a 1/8" stainless line for the Picarro (~200 ccm flow rate), and a ¼" Teflon line for the ethane spectrometer (~4 l/min flow rate). This results in lag times of ~5 seconds for the ethane and ~10 seconds for the Picarro. The lag time for the Picarro is calculated using a "breath" test with the CO2 measurement, and the ethane lag time is adjusted to maximize the correlation between it and the Picarro methane time series in plumes where both gases are emitted.

CHAPTER 2:
Source Quantification using Gauss's Theorem

2.1 Theory

The research group uses an integrated form of the scalar budget equation to estimate the emission of a gas of interest within a cylindrical volume V circumscribed by a series of closed aircraft flight paths (typically circular) flown around the source over a range of altitudes from the lowest safe flight level, usually 150 m (agl), to an altitude where no discernable change in the trace gas density c is observed around the flight loop, zmax. The research group begins with the integral form of the scalar budget equation for a chemically unreactive species, $c = C + c'$, where C is the mean mixing ratio around each circle and c' is the departure from the mean.

Figure 1 shows the plume dispersion envisioned here. Effluent is emitted from a source on or near the surface and carried downwind as it mixes upward. An imaginary surface is assumed enclosing the source and extending above the vertical extent of the plume so that there is no vertical transport through the top of the imaginary volume.

Figure 1: Schematic of Dispersion from Surface Source

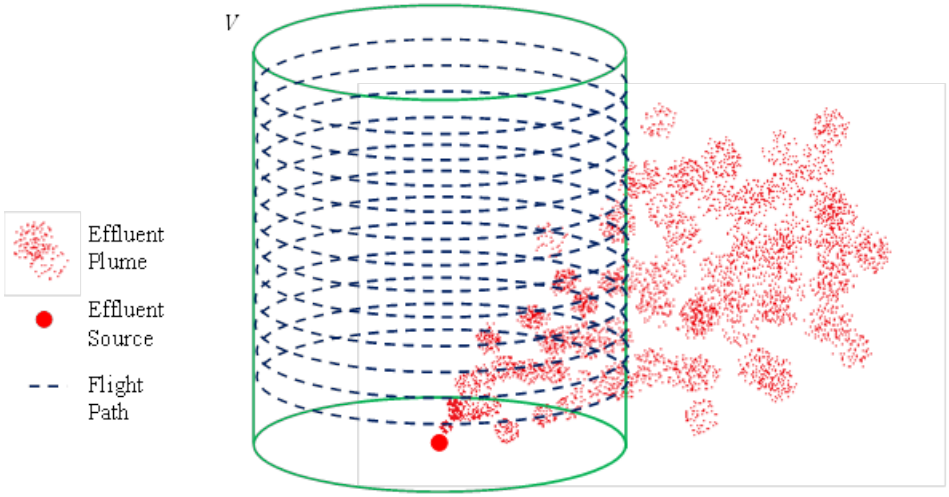

To estimate the source strength, the research group starts with the integral form of the continuity equation:

$$\langle\frac{\partial m}{\partial t}\rangle + \iiint \nabla \cdot F_c dV = Q_c \quad (1)$$

where F_c is the flux of c, Qc is the sum of the internal sources and sinks of c within V and m is the mass of c.

Next, the research team use Gauss's theorem to relate the volume integral to a path integral around the aircraft's flight path.

$$Q_c = \langle \frac{\partial m}{\partial t} \rangle + \iiint \nabla \cdot F_c dV = \left\langle \frac{\partial c}{\partial t} \right\rangle + \oint F_c \cdot \hat{n}\, dS \qquad (2)$$

where S is the surface enclosing V and $\hat{n}$ is an outward pointing unit vector normal to the surface.

The surface integral can be broken into three elements: a cylinder extending from the ground up to a level above significant modification by the emission, the ground surface circumscribed by a low-level (virtual) circular flight path (z = 0), and a nominally horizontal surface circumscribed by a flight path above the level modified by the source ($z = z_{max}$). The flux into the ground is negligible and since z_{max} is above the level to which contribution from surface emission extends, the flux through the top surface is similarly negligible. Thus,

$$\oint F_c \cdot \hat{n}\, dS = \int_0^{z_{max}} \oint c\overrightarrow{u_h} \cdot \hat{n} dl\, dz \qquad (3)$$

where $u_h = u\mathbf{i}+v\mathbf{j}$.

For a case where the source strength Qc is insufficient to raise the downwind concentration measured by the aircraft by more than a few percent above the background, the first term on the right side of Eq. 4, which is the total mass divergence times the mean concentration may overwhelm the contribution of the second term and be significantly in error because of the difficulty in obtaining an accurate estimate of the divergence, which is normally very small [Lenschow et al., 2007]. The research team performs a scale analysis of the terms in that make up the path integral in Eq. 4:

$$\oint c\overrightarrow{u_h} \cdot \hat{n} dl\, dz = \iint \nabla_h \cdot cu_h dA = \iint (u_h \cdot \nabla c + c\nabla \cdot u_h)\, dA \qquad (4)$$

The last term is the concentration multiplied by the divergence of the wind field. The research group assumes here that the plume mixes vertically and laterally at a fixed rate of 1 m s^{-1}. The results are shown in Table 1 and, for all but the most extreme conditions, the divergence term is at least an order of magnitude smaller than the gradient term. The research team note this limitation of the method for small leaks (< 10 kg hr^{-1}) and very light winds (~ 1 ms^{-1}).

Table 1: Comparison of Terms in Scalar Budget Equation

Leak Rate kg hr^{-1}	Wind Speed m s^{-1}	$\vec{u} \cdot \nabla c$ kg m^{-4}	$c\nabla \cdot \vec{u}$ kg m^{-4}	Ratio
100	5	6.94E-10	1.15E-12	0.002
100	2	1.11E-10	1.15E-12	0.010
100	1	2.78E-11	1.15E-12	0.041
10	5	6.94E-11	1.15E-12	0.017
10	2	1.11E-11	1.15E-12	0.104
10	1	2.78E-12	1.15E-12	0.414

Except in conditions of lite winds and small leak rate, the divergence term is much smaller than the gradient term.

Mathematically, the divergence term is eliminated by removing the mean concentration. For a species like methane, the mean mixing ratio (~2000 ppb) is an order of magnitude larger than the normal deviations

of a few hundred ppb allowing us to eliminate most of the divergence term just by subtracting off the mean mixing ratio. This subtraction has no effect on the gradient term.

$$c\nabla \cdot \vec{u} = (C + c')\nabla \cdot \vec{u} \qquad (5)$$

For other gases, such as ethane, the deviations are as large or larger than the mean, and the research team is left with the imprecise divergence error in our calculation. If the estimates of the divergence are assumed to be an order of magnitude high, they will amount to a 10% error for a small source (10 kg hr^{-1}) in a moderate wind (5 m s^{-1}).

$$Q_c = \langle \frac{\partial m}{\partial t} \rangle + \int_0^{z_{max}} \oint c' \overrightarrow{u_h} \cdot \hat{n} dl \, dz \qquad (6)$$

2.2 Choosing the Downwind Sampling Distance

The optimal sampling distance from the targeted point source is a trade-off between signal to noise ratio and a predictable shape of the plume near the surface. Very close to a source, the flux divergence profile exhibits a strong gradient below the minimum safe flight altitude, making that term difficult to estimate, as shown in Figure 2. Very far from a source, the signal becomes obscured by instrument and atmospheric variability.

Figure 2: Flux Divergence Profiles Generated from WRF-LES Runs

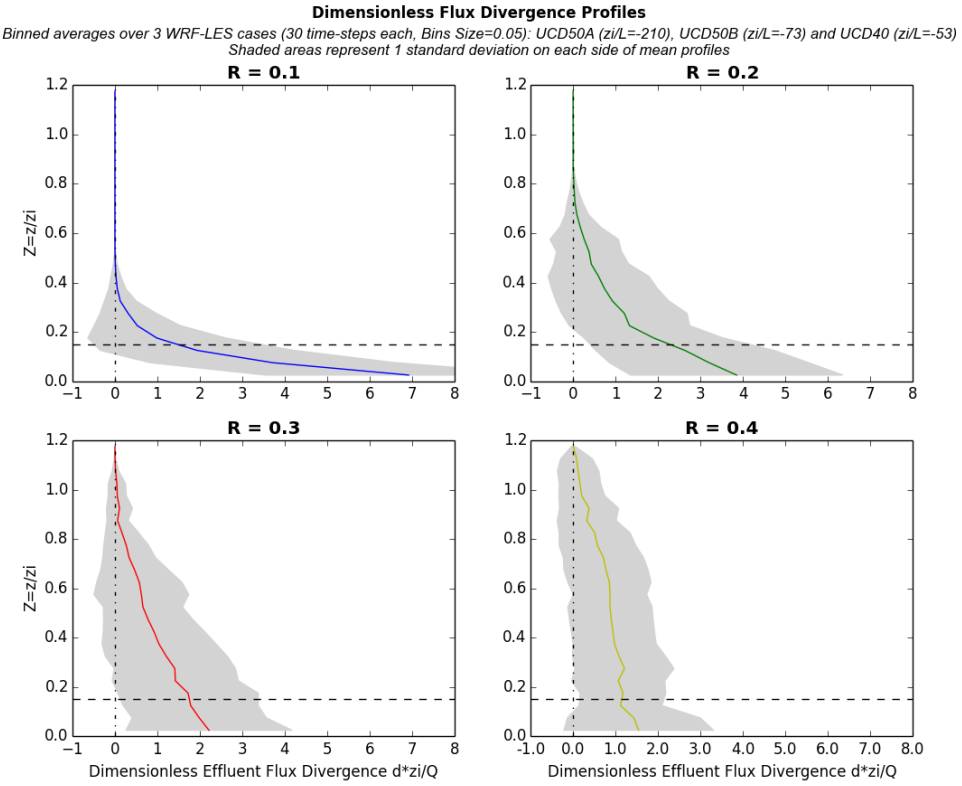

The research group seeks to select a distance are enough to allow sufficient mixing yet close enough so that plume crossings are easily observable against the background variability and instrument noise. This distance is expressed in terms of the dimensionless downwind distance R [Willis and Deardorff, 1976].

$$R = \frac{xw_*}{Uz_i} \qquad (6)$$

Where x is the downwind distance, w* is the convective velocity scale, zi is the boundary layer height and U is the mean wind speed.

To investigate this distance dependence, the research team ran numerical simulations using WRF-LES, modified to simulate a continuous surface source, as shown in Figure 2. These results suggest an optimal distance near R = 0.5 in the vertical region $z/z_i = 0.15$. In this region, the flux in the bottom altitude bin can simply be extended to the surface by extrapolating the flux from the lowest altitude aircraft circular path.

2.3 Minimum Number of Passes

The atmospheric boundary layer is a turbulent medium, meaning that two passes at the same distance and altitude will likely see different measurements. The research team investigates the number of passes required to obtain a statistically robust estimate. First, the research team employs LES and then calculates the fluxes as if the research group had an airplane flying through the simulated field. The research team then randomly samples the fluxes from each of the legs and plots the estimated emission rate as a function of the number of samples used as shown in Figure 3. Next, the research team analyzes actual flight data from an ethane controlled release and those results are shown in Figure 4. What is evident from both cases is that somewhere around 15 passes is sufficient to estimate the emission rate.

Figure 3: LES Study of Leak Rate versus Number of Laps

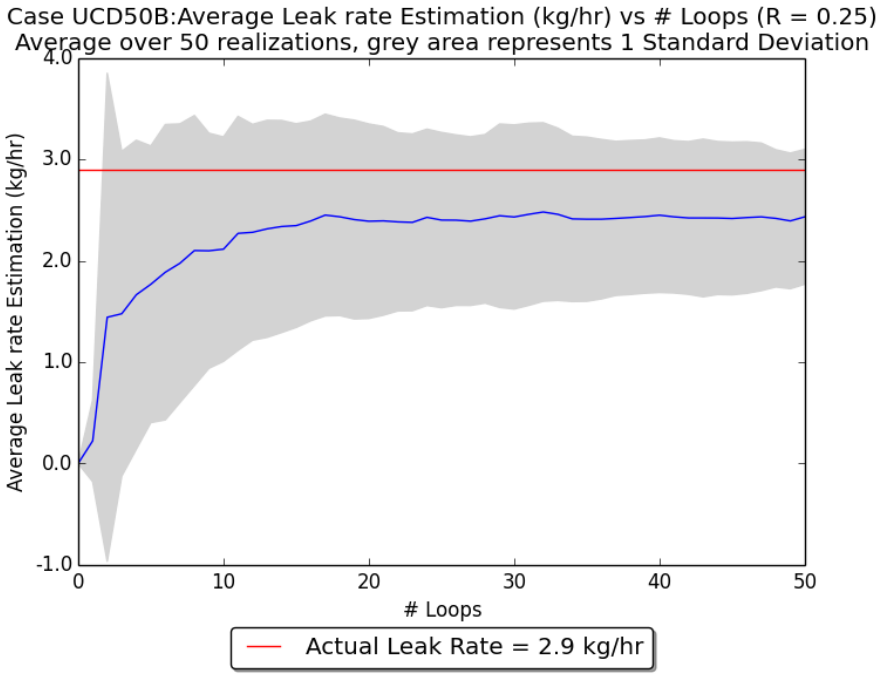

Figure 4: Leak Rate from Random Samples

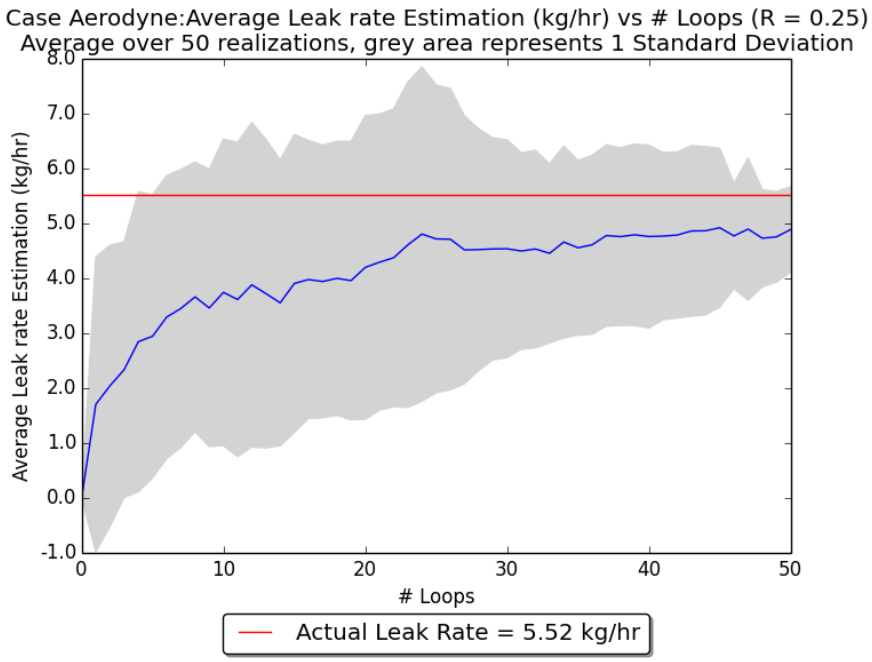

Individual legs from the Aerodyne controlled release in Denver on November 19, 2014.

2.4 Altitude Binning the Flux Divergence Data

If all altitudes were sampled equally, the total divergence could be calculated by averaging the laps at all altitudes and then multiplying by the top altitude. In practice, the plume exhibits much more variability close to the surface, meaning more laps are required in that region than above. To ensure that all altitudes are equally weighted, the research team divides the vertical range into six equally spaced bins, and averages the measurements from the laps within each bin. The total emission is the sum of the flux in each bin multiplied by the bin width. The research team also performed six flights where the research team sampled equally at all altitudes, allow a comparison of the direct average versus the binned results. The two values agreed to within 5%.

2.5 Error Analysis

The research team assumes the source has reached quasi-steady state before our measurement. The leg to leg variability is primarily driven by the stochastic nature of turbulence (e.g. the research team hit the plume one lap, miss it another). By dividing the laps into vertical bins, the research team can use the standard deviation of the points within the bin as an estimate of the uncertainty within that bin. Then the total uncertainty in the estimate of the flux divergence is simply estimated by adding up the individual bins in quadrature.

The next term is the time rate of change of the scalar density. This is estimated by performing an ordinary least squares fit, using time and altitude as the predictors and the methane mixing ratio as the response variable, i.e.:

$$c = \alpha t + \beta z \qquad (7)$$

The uncertainty in the term α (usually expressed in units of ppb hr^{-1}) is then converted to density units using the average pressure and temperature for the cylinder and multiplied by the volume of the cylinder to obtain the uncertainty in the rate of change of the total scalar mass within the cylinder.

Finally, the two uncertainties (time rate of change, flux divergence) are combined to obtain the total uncertainty in the flux estimate. The flux profile for the first Aerodyne test is shown in Figure 5. Each of the blue dots represents an individual path around the site.

Figure 5: Ethane Flux Profile for Aerodyne

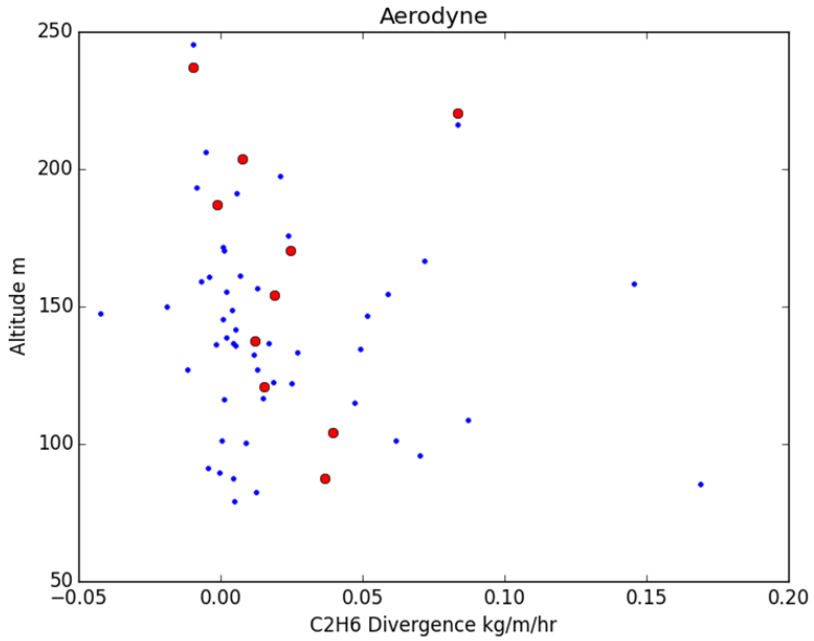

Controlled release on November 19, 2014.

After the individual passes have been binned into the desired number of bins, the standard deviation of the points in each bin is calculated. Figure 6 shows the vertical profile observed during the Aerodyne test. The typical minimum allowable altitude (150 meters) is depicted and shows considerable variability below that point.

Figure 6: Ethane Flux Profile - Second Aerodyne Controlled Release

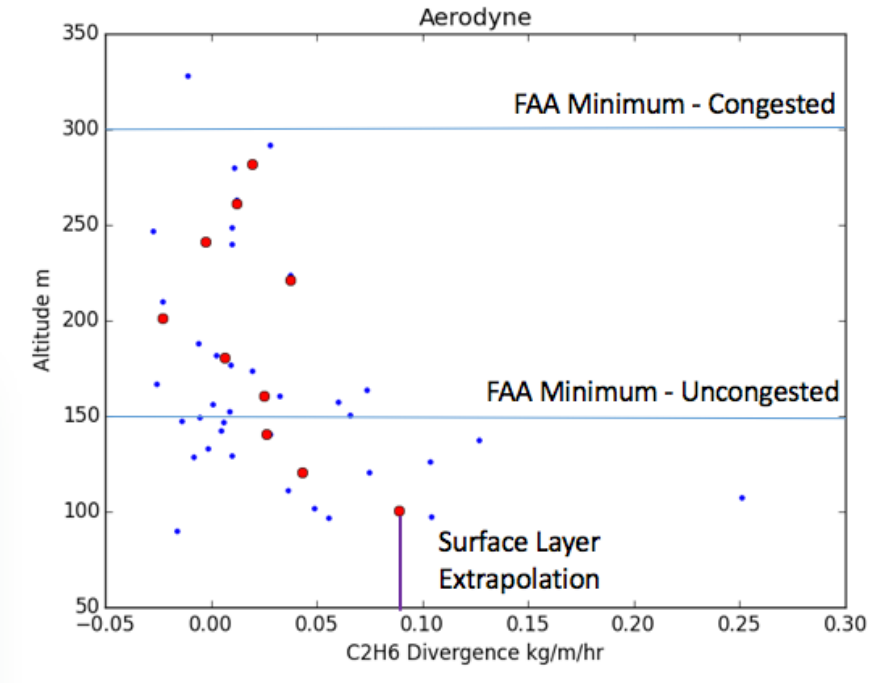

Second Aerodyne controlled release on October 3, 2015 in Bee Branch, Arkansas. The two thin blue lines depict the typical minimum flight altitudes for congested and uncongested areas, as defined by the FAA. The thicker purple line shows the typical surface extrapolation but clearly suggests that would not work with a minimum altitude of 150 or 300 meters.

2.6 Results

The research team uses three types of flights to characterize the accuracy of this estimation method. The research team performed six days of flights with a natural gas controlled release supported by the Pacific Gas & Electric Company (PG&E), two days with an ethane controlled release provided by Aerodyne, and six power-plant flights where our estimates are compared with reported CO_2 emissions.

2.6.1 Power Plant Flights

Power plants in the U.S. are required to report CO_2 emissions to EPA (https://ampd.epa.gov/ampd) on an hourly basis. The accuracy of the reported CO_2 emissions have been determined to be ±10.8-11.0% resulting from reported U.S. average differences between EIA fuel-based estimates and EPA continuous emission monitoring based estimates [Ackerman and Sundquist, 2008; Peischl et al., 2010; Quick, 2014]. Also, Peischl determined an accuracy of power plants reported CO_2 emissions in Texas of ±14.0% based on differences between observed downwind SO_2/CO_2 and NOx/CO_2 emission ratios and those reported via EPA continuous emission monitoring [Peischl et al., 2010].

The research team uses the slightly larger uncertainty from Peischl et al. An additional uncertainty arises from temporal emission variability (hourly average reported CO_2 emissions versus <1 hour power plant flights that may cover parts of two reported consecutive hourly values). The research team estimates the

total reported uncertainty by summing in quadrature the Peischl estimate and the relative difference between two reported consecutive hourly values during each flight. The aircraft frequently encountered power plants during oil & gas monitoring campaigns, but usually did not have the flight time to perform a full emissions characterization of the power plant.

The research team limits the comparison to days when the aircraft performed a minimum of 10 laps around the plant, excluding the quick fly-bys where uncertainties would be unacceptably large. The results are presented in Table 2 and indicate very good agreement between Gauss's method and the reported CO_2 emissions with the averaged magnitude of the difference being 10.6%. Power plant emissions are "hot" gases and much more buoyant, so different from a surface emission source that isn't combustion related (or otherwise heated).

Table 2: Power Plant Estimates

Power Plant	Date	Hour UTC	Laps	Reported T hr^{-1}	Estimated CO_2 kg hr^{-1}	Difference
Rocky Mountain Energy	10/06/14	20	19	99±14	111±24	13%
Saint Vrain	10/04/14	19	21	124±17	122±41	-1%
Pawnee	11/19/14	20	14	575±81	555±160	-3%
Saint Vrain	09/17/15	20	14	361±54	280±115	-23%
Four Corners Power Plant	04/11/15	18	12	1289±387	1119±343	-13%

2.6.2 Ethane Controlled Releases

Two experiments with known ethane releases were performed in collaboration with Aerodyne. The actual release rate was measured with a flowmeter by the Aerodyne ground crew. The Denver site was located in a remote area approximately 105 miles NW of Denver. This site was chosen because of the flat terrain and lack of other nearby ethane sources that could complicate the measurement. Agreement was excellent with the estimate falling within 10% of the actual release rate. The second Aerodyne controlled release (OCT2015) was performed at a site surrounded by active oil & gas extraction operations and complex terrain. The ethane flux estimate is 25% higher than the actual release rate and the calculate uncertainty is significantly higher than the research team has seen on other sites (Table 3).

One interesting result of this test was the presence of a significant upwind ethane source. This source was evident on roughly half of the upwind passes, suggesting that techniques which rely on a limited number of upwind passes to characterize the background would likely have missed that source and, since it was upwind of the main source, it would be included in the emission estimate. The same problem would affect those techniques that employ a downwind transect, using the edges of that transect to estimate the background concentration.

Table 3: Ethane Controlled Release

Test Name	Date	Laps	Actual Methane kg hr^{-1}	Estimated Methane kg hr^{-1}	Actual Ethane kg hr^{-1}	Estimated Ethane kg hr^{-1}
Denver	11/19/14	50	0.0	4.9±2.3	5.6±0.5	6.0±3.0
OCT2015	10/03/15	19	0.0	-3.4±12.3	8.1±0.8	10.1±6.1

2.6.3 Natural Gas Controlled Releases

In conjunction with the Pacific Gas & Electric Company, the research team performed a total of four days of controlled release experiments, exactly one year apart. The first set was performed southeast of Sacramento near the town of Rio Vista and the second set near Bakersfield, California at the Rio Vista "Y" station (Table 4). The release rate was not calibrated with a flow meter but, based on the size of the orifice and the upstream pressure, the release rate is estimated at 15.2 kg hr-1. This release rate is an estimate of the total gas being released which is a combination of primarily methane and ethane. The research group uses the regression fit of ethane to methane (averaging 0.085 by mass) to estimate the actual release rate of each scalar.

The methane controlled releases suffer from the relative amount of enhancement versus the total in the air. During the Bakersfield release, the largest signal the research team saw was 100 ppb, with 30-40 ppb being more common. Using a typical background level of 2 ppm, this enhancement represents 2% of the background. Things are much brighter for ethane where the research group the enhancements are as large as or larger than the background.

Table 4: Natural Gas Controlled Release

Site	Date	Laps	Actual Methane kg hr^{-1}	Estimated Methane kg hr^{-1}	Actual Ethane kg hr^{-1}	Estimated Ethane kg hr^{-1}
Rio Vista	11/03/14	127	13.9±2.8	14.2±7.5	1.2±0.5	1.1±0.6
Rio Vista	11/04/14	132	13.9±2.8	11.9±15.6	1.2±0.5	1.1±0.5

CHAPTER 3:
The Aliso Canyon Blowout

3.1 Introduction

On October 23, 2015, a major natural gas leak of indeterminate size was reported in the Aliso Canyon area and was later identified as originating from SS-25, one of 115 wells connected to the subsurface storage reservoir. Processed natural gas is composed primarily of methane (CH_4), a powerful greenhouse gas, and ethane (C_2H_6), both of which can lead to background tropospheric ozone production; at sufficiently high concentrations, natural gas leaks pose an explosion hazard and, if inhaled, can induce nausea, headaches, and impaired coordination. Exposure to odorants that are added to natural gas, which are typically sulfur-containing compounds such as tetrahydrothiophene [$(CH_2)_4S$] and 2-methylpropane-2-thiol [t-butyl mercaptan;$(CH_3)_3CSH$] can cause short-term loss of the sense of smell, headaches, and respiratory tract irritation.

Major natural gas leaks therefore can have adverse impacts on climate, air quality, and human health. This incident highlights the utility of rapid-response airborne chemical sampling in providing an independent, time-critical, accurate, and spatially and temporally resolved leak rate, as well as in ascertaining the source location and plume chemical composition. Such information can help to document human exposure, formulate optimal well-control intervention strategies, quantify the efficacy of deliberate control measures, and assess the climate and air quality impacts of major unanticipated chemical releases to the atmosphere [M. K. McNutt et al., 2012; T. B. Ryerson et al., 2012]

3.2 Quantification of Methane and Ethane Emissions

Ground-based whole-air sampling (WAS) with stainless steel canisters on 23 December 2015, followed by laboratory analysis, provided information on the chemical speciation of the leaking hydrocarbon mixture. The analysis quantifies a massive CH_4 release using a rapid, direct, and repeatable method with known accuracy. As such, results from this method serve as reference values for less direct and timely estimates that use retrievals of surface [R. A. Washenfelder, 2003; K. W. Wong et al., 2015], airborne [R. O. Green et al., 1998], and/or satellite remote sensing observations [A. Butz et al., 2011].

These data show that over its 112-day duration, the Aliso Canyon natural gas leak released a total of 97,100 metric tons (5.0 billion SCF) of CH_4 (Figure 7) and 7300 metric tons (0.2 billion SCF) of C_2H_6 to the atmosphere, which is equal to 24% of the CH_4 and 56% of the C_2H_6 emitted each year from all other sources in the Los Angeles basin combined [J. Peischl et al., 2013]. This CH_4 release is the second largest of its kind recorded in the United States, exceeded only by the 6 billion SCF (115,000 metric tons) of natural gas released in the 2004 collapse of an underground storage facility in Moss Bluff, TX, and greatly surpassing the 0.1 billion SCF (1900metric tons) of natural gas leaked from an underground storage facility near Hutchinson, KS, in 2001 [B. Miyazaki, 2009].

Figure 7: Aliso Canyon Gas Plume Transport into Populated Areas

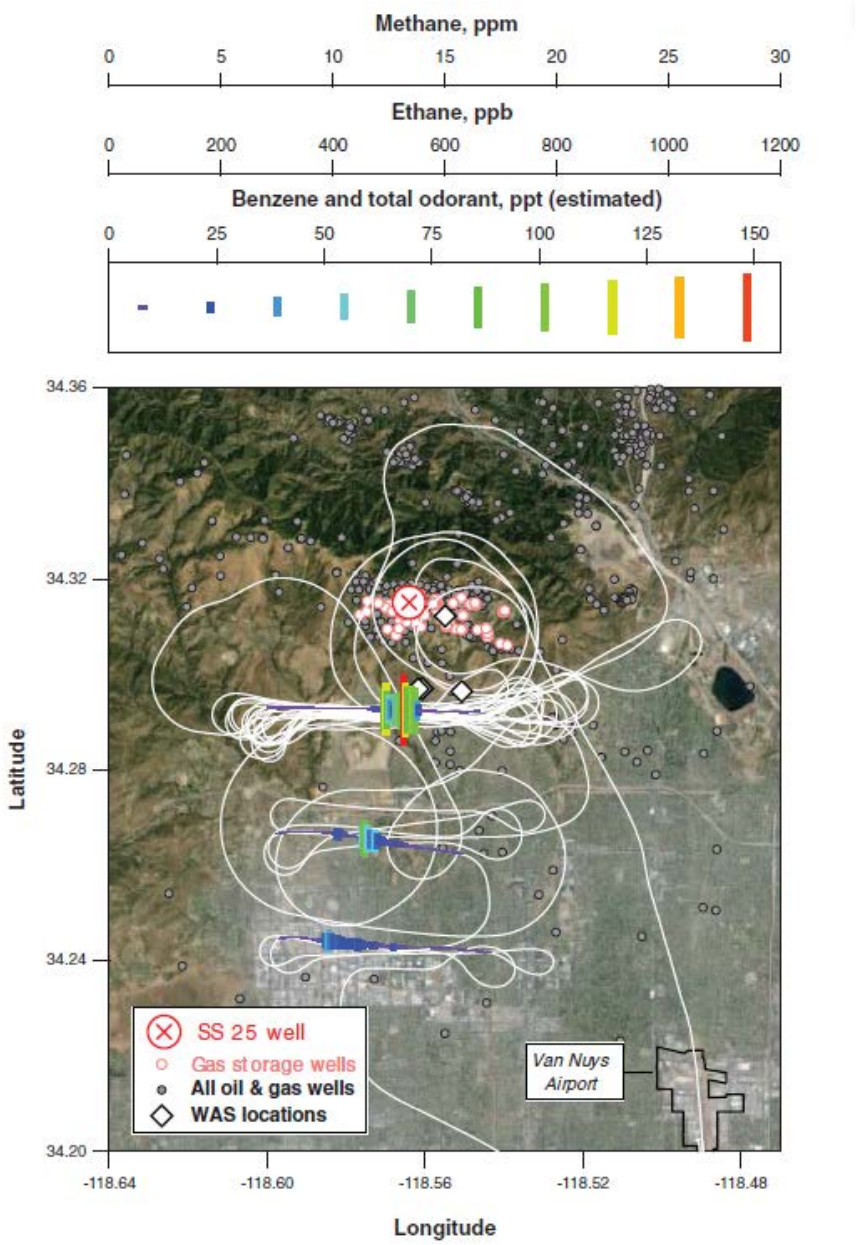

3.3 Other Potential Chemicals of Concern

Trace enhancements of benzene, toluene, ethylbenzene, and xylene isomers (the so-called BTEX compounds) were also detected at ratios of 0.001% or lower relative to CH_4. Benzene is a known human carcinogen [U.S EPA, 2014]; thus, population exposure to benzene from the Aliso Canyon leak has received particular attention. Trace enhancements of benzene, toluene, ethylbenzene, and xylene isomers (the so-called BTEX compounds) were also detected at ratios of 0.001% or lower relative to CH_4 (table S1). Benzene is a known human carcinogen [U.S EPA, 2014]; thus, population exposure to benzene from

the Aliso Canyon leak has received particular attention. Composition data from the WAS canisters indicate a benzene-to-CH_4 enhancement ratio of $(5.2 \pm 0.1) \times 10^{-6}$ (uncertainties throughout are ±1 SEM), which is broadly consistent with an ER of $\sim 7 \times 10^{-6}$ found in highly concentrated samples that were collected ~3 m downwind of the SS-25 well site [South Coast Air, 2016]. Together, these samples suggest minimal variation over time in the benzene composition of the leaking gas.

CHAPTER 4:
Detecting Pipeline Leaks

4.1 Introduction

Natural gas transmission lines carry high pressure (~500 PSI) over long distances, often through rural areas, making them ideal for fixed wing aircraft. Unfortunately, the speed of fixed wing aircraft is also their Achilles heel, as narrow plumes and sharp turns in the pipeline can pose significant challenges to the leak detection process. Given the fractional operating cost of fixed wing versus rotor, a major goal of this project was determining the effectiveness of fixed wing aircraft, specifically in the realm of detecting and quantifying leaks from natural gas transmission lines.

For this project, the research team added another discriminator to the mix, ethane. The primary source of ethane globally is natural gas deposits. Little ethane is emitted by dairies, landfills and other typical methane sources. While the presence of ethane does not guarantee the source is on the pipeline, it does exclude the vast majority of non-oil and gas sources.

4.2 General Principles

Any gas released into the atmosphere will ultimately mix in with surrounding air and be carried along by the local wind. The mixing process is primarily driven by turbulent transport and is governed by the equation for turbulent kinetic energy (TKE). The primary drivers for turbulence are wind shear and stability. For a surface release to be detected from a safe flight level, the turbulent transport must act to lift the gas to that level (~150 meters), and that lifting must occur before the plume has become so diluted that it becomes difficult to distinguish from the background.

Figure 8 shows the state of the research prior to this project. The blue line is the transmission line (in this case, Mineral Wells, Texas) and the small circles represent methane enhancements detected along the aircraft's flight path (well downwind of the pipeline). The magenta pie wedges indicate the likely source of the enhancement, estimated by a rudimentary back-trajectory using the wind measured at the aircraft. What the research group learned from this and other projects was that detecting the enhancement wasn't the challenge, determining the source (pipeline, cows, landfills, etc.) was.

Figure 8: Transmission Line Test over Mineral Wells, Texas

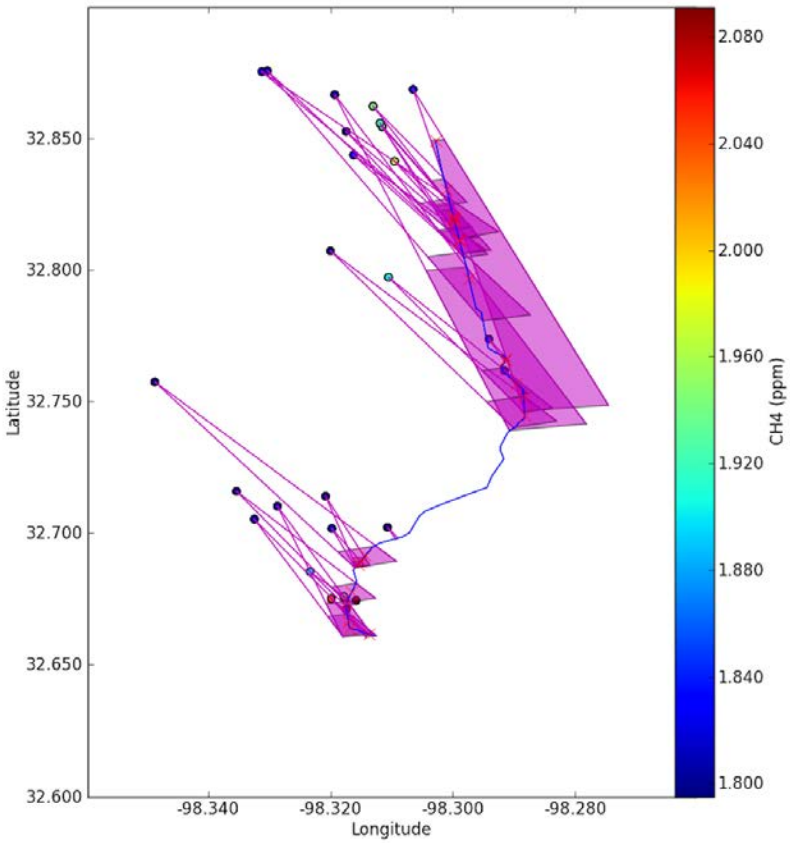

Pipeline shown in blue.

The three primary challenges to detecting pipeline leaks from aircraft are:

1. Flying at the optimal location to intercept the plume and
2. Determining the position on the pipeline of the source that caused the plume
3. Understanding the meaning of a non-detect.

4.3 Optimal Downwind Distance

To determine the optimal location, the research team used large eddy simulation (LES) to simulate a surface release under varying atmospheric conditions. The results of one of those cases are shown in Figure 9 and indicate that, for a typical boundary layer height (~1 km), using a minimum safe altitude of 150 meters (500 feet), beyond a dimensionless distance of ~0.25, the research team has a very high probability of passing through the plume. Assuming a 5 m s^{-1} wind speed, and a 1 m s^{-1} convective scaling velocity (w*), this translates to a minimum downwind distance of:

$$x = \frac{XU\ z_i}{w^*} = \frac{(0.25)(5\ m\ s^{-})(1000\ m)}{1\ m\ s^{-1}} = 1.25\ km$$

The research team seeks to fly at the minimum distance because as the distance grows, the enhancement shrinks. For a small leak, downwind enhancements quickly blend into background values.

Figure 9: LES Simulation Showing Flux Divergence versus Height

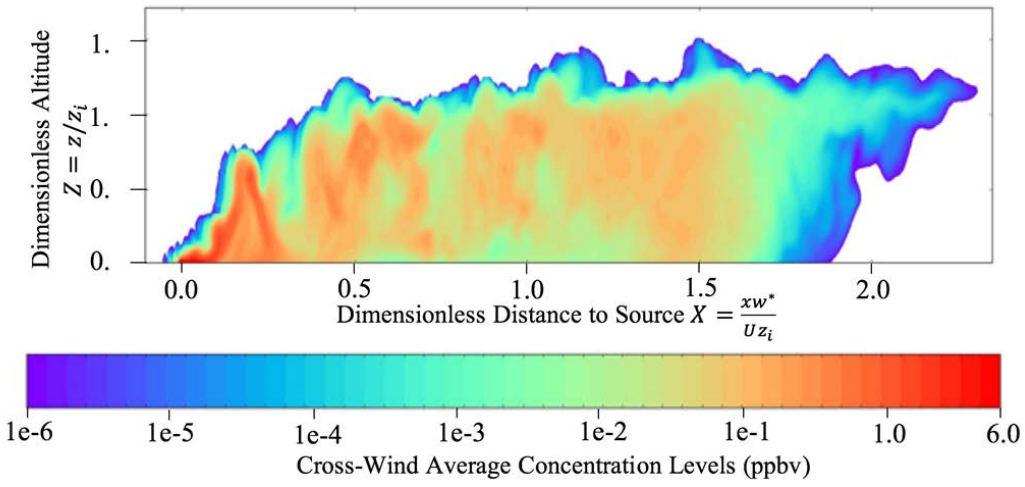

4.4 Determining Source Location

Once a methane enhancement has been detected, and confirmation provided by corresponding ethane enhancement, the research team seeks to identify the likely location on the pipeline from which the methane originated.

To investigate this, the research team creates a virtual pipeline running through a known release, perpendicular to the mean wind. The research group uses flight data from May 25, 2016 for this purpose. This flight was conducted around the Princeton Gas Storage facility, known to have a consistent leak of approximately 30 kg hr^{-1}. The average of the indications falls within 25 meters of the center of the facility, and the farthest point is 600 meters away (Figure 10). The research team can estimate the expected error by examining the standard deviation of the wind direction. Since the wind is evolving in time, the research group looks at 10 minute segments, and then averages the standard deviation of all the segments. For this flight, that yields a standard deviation of 60 degrees. From 1 km away, a 60 degree error would translate into a predicted uncertainty along the pipeline of 1000 meters.

Figure 10: Princeton Test Flight

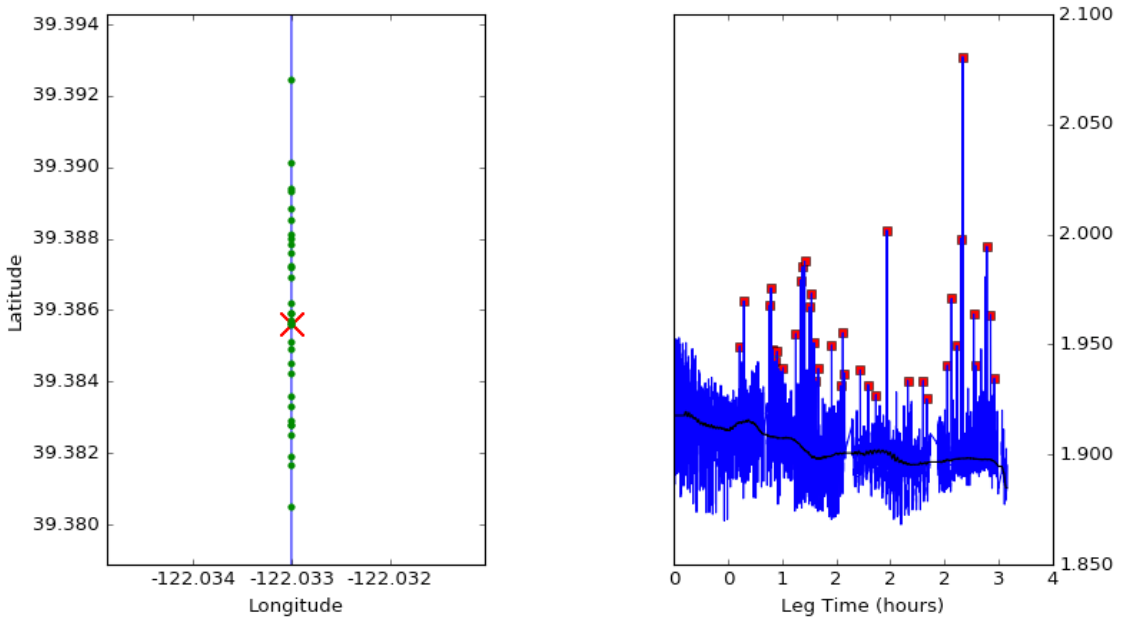

In this case, the research team flew ~100 laps around the Princeton gas facility and then uses the momentary wind direction to back-track the enhancement to its likely location on the pipeline. The green dots on the left panel indicate the position of each "source". The large red "X" marks the center of the Princeton Gas Field.

4.5 Pipeline Leak Test Flights

The September 15, 2016 flight was spent investigating sources identified by the JPL flight. The research team visited three of the sources identified; Honor Rancho, Chino Hills and the Newberry Compressor (Table 5).

Table 5: September 15, 2016 Flight

Site	Location	Date	Methane (kg hr^{-1})	Unc (kg hr^{-1})	Ethane (kg hr^{-1})	Unc (kg hr^{-1})
Honor Rancho	34.460N 118.594W	9/15/16	60.6	205	12.3	10
Chino Hills	33.940N 117.720W	9/15/16	0	10	0	0.5
Newberry Compressor	34.7804N 116.596W	9/15/16	66.9	14.9	3.6	0.9

On September 12, 2016, the research team flew the pipelines in the SJV circling where the research team found enhancements. Four methane enhancements were noted and quantified (Table 6). Without confirmation from ground teams, the research team can't be sure of the precise leak location (and if it is truly a pipeline leak). The Oak Flat compressor was very noisy, which is often caused by an intermittent source, but despite the high uncertainty (statistically no different from zero), the research team observed an enhancement there, so there is a leak, despite our inability to quantify it.

Table 6: September 12, 2016 Flight

Site	Location	Date	Methane (kg hr^{-1})	Unc (kg hr^{-1})	Ethane (kg hr^{-1})	Unc (kg hr^{-1})
Panoche Energy Center	36.652N 120.581W	9/13/16	140.0	15.7	1.8	0.3
Fink Road Landfill	37.386N 121.137W	9/13/16	94.4	23.8	0.1	0.1
Oak Flat Rd Compressor	37.422N 121.150W	9/13/16	18.4	47.6	0.5	0.5
Tracey Biomass Plant	37.715N 121.491W	9/13/16	136.4	27.3	3.3	0.9

While flying the pipeline on September 11, 2016, a large enhancement was detected near Willows, California (Table 7). The pilot immediately began the procedure to localize the leak, flying legs perpendicular to the wind, moving gradually upwind until the signal vanished. The location of the source was the Wild Goose Storage LLC Compressor station. This facility had not been included in previous estimates of the Wild Goose Storage emissions because it was not listed in the DOGGR database, and was 6 km away from the listed sites.

Table 7: September 11, 2016 Flight

Site	Location	Date	Methane (kg hr^{-1})	Unc (kg hr^{-1})	Ethane (kg hr^{-1})	Unc (kg hr^{-1})
Wild Goose Storage Compressor Station	39.348N112 1.819W	9/11/16	143.3	38.0	10.6	3.7
Farmers Rice Coop	39.359N 122.029W	9/11/16	0	5	0	0.5

The Wild Goose Storage Compressor was located by flying a “snake” pattern from where the plume was first detected, as shown in Figure 11.

Figure 11: Snake Pattern Flown - Wild Goose Storage Compressor Station Source

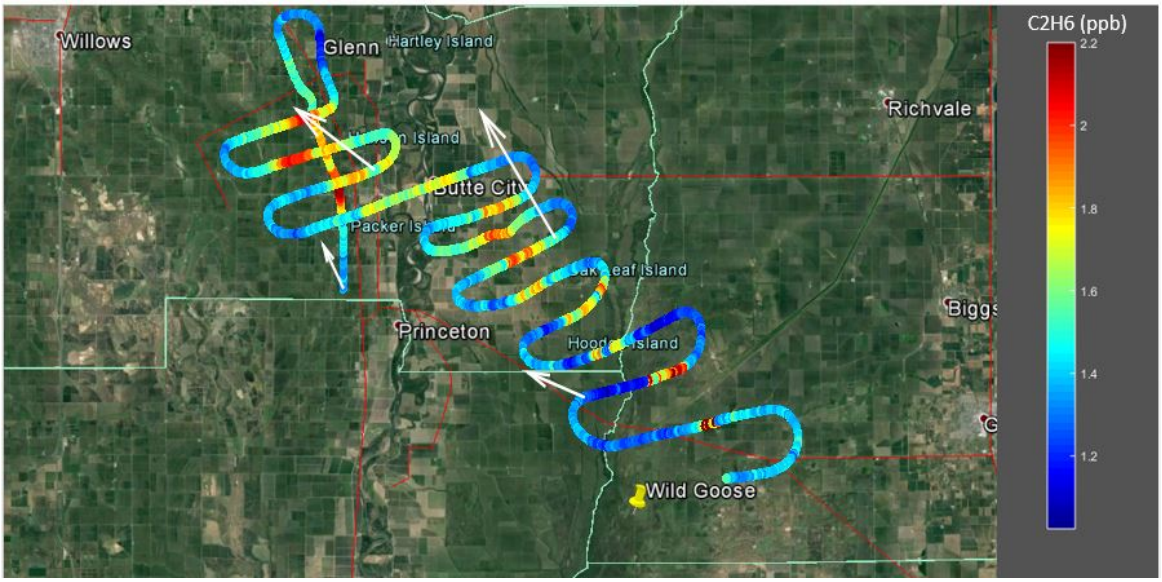

The September 10, 2016 flight was primarily a pipeline flight, with the addition of a compressor station where the research team observed a strong enhancement of both methane and ethane (Table 8).

Table 8: September 10, 2016 Flight

Site	Location	Date	Methane (kg hr^{-1})	Unc (kg hr^{-1})	Ethane (kg hr^{-1})	Unc (kg hr^{-1})
Burney Compressor	40.898N 121.636W	9/10/16	86.7	18	6.4	1.5

The September 9, 2016 flight included pipelines in northern California.

Additionally, the research team located a likely pipeline leak, as shown in Figure 12.

Figure 12: Likely Pipeline Leak Detected on September 11, 2016

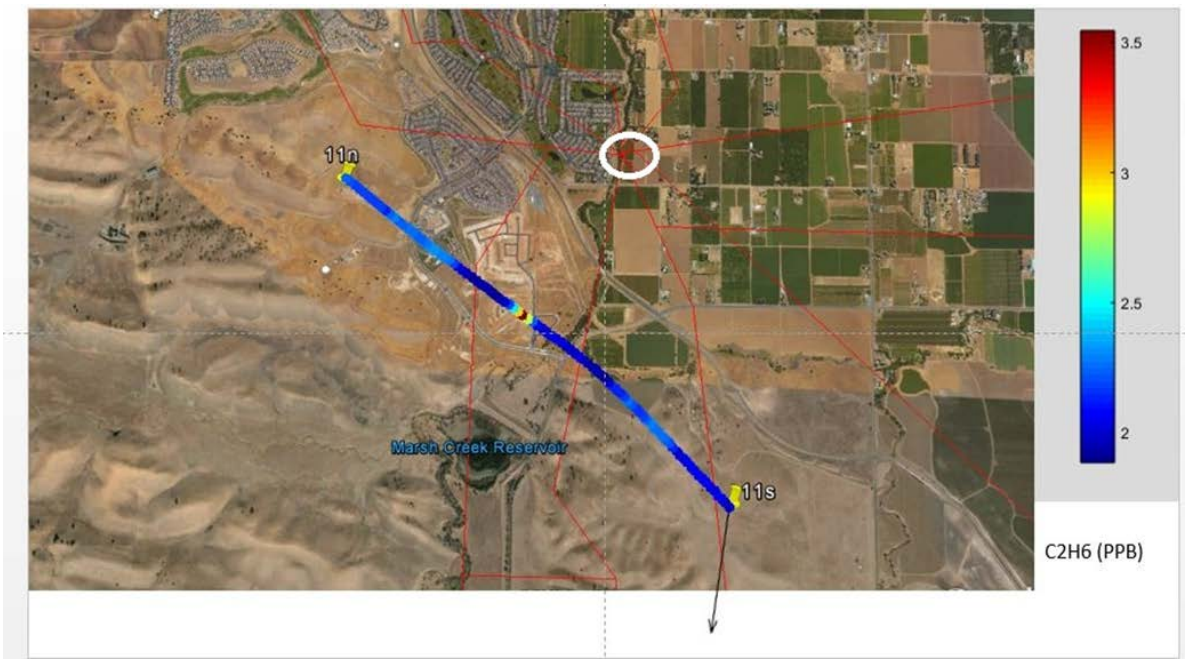

The pipeline sources discovered during the final flights are tabulated in Table 9.

Table 9: Tabulation of Emission Sources Discovered During Pipeline Flights

Date	Spike Time (s)	Max Ethane Enhancement (ppb)	Plume width (m)	Source lat	Source long
8/25/2016	7.5	0.7	570	39.1598	-122.0735
9/2/2016	6.5	0.8	463	36.6507	-120.5847
9/2/2016	3	0.65	240	34.8306	-116.6786
9/3/2016	4.5	0.6	364	37.3038	-121.0773
9/3/2016	9	0.9	728	37.7167	-121.4902
9/3/2016	6	1.1	533	38.1483	-121.6293
9/6/2016	3	0.5	232	40.0629	-122.2141
9/9/2016	10	2	834	37.786	-121.2508
9/9/2016	2.5	0.4	199	37.3124	-120.5106
9/9/2016	6	2.2	456	36.7885	-119.9137
9/9/2016	25	2	1804	36.591	-119.6339
9/9/2016	18	1.6	1291	36.5938	-119.634
9/9/2016	3.5	1.7	257	36.6499	-119.7103
9/9/2016	3	14	223	36.1469	-120.3872
9/9/2016	10	2.5	747	36.1469	-120.3872
9/9/2016	2.5	1.8	202	36.0711	-120.0478
9/9/2016	3	1.5	218	37.9055	-121.7148

4.6 Non-Detect Confidence

The goal with pipeline detection is to calculate an appropriate downwind distance which will maximize the probability of plume intercept at the aircraft's altitude. Ideally, for flight safety, the aircraft would fly at or above 150 meters (500 feet). The first question the research team asks on the pipeline detection is how many passes would be required to confidently assert that a non-detect implies no leak. To investigate this, the research group went to a site with a known moderate leak (~35 kg hr^{-1}), which the research group has repeatedly measured and flew 112 laps around the facility, all at 500 feet (150 meters) (Figure 13).

The research team set the threshold for spike detection at 2 standard deviations above the mean methane mixing ratio. Using that threshold, we encountered the plume on 75 out of the 112 laps, giving a detection probability of 67%. For any pass, there is a 33% probability that the research team misses the plume, meaning that the probability of missing 3 consecutive passes is $(0.33)^3 = 0.04$. This means that if the research group has 3 consecutive passes without observing a spike, the research group can say with 96% confidence that there is no leak of this magnitude.

Figure 13: Princeton Underground Storage Facility

112 laps were flown to investigate the variability in source localization and the likelihood of an erroneous non-detect.

CHAPTER 5:
Detecting Leaks in Underground Storage Facilities

The California Energy Commission in collaboration with the Air Resources Board envisioned and supported a coordinated research effort to survey methane emissions from the natural gas system from wells to final consumption. In response to the Aliso Canyon natural gas leak incident, the California Energy Commission asked Scientific Aviation, a member of the research team, to conduct a number of airborne flight measurements to quantify the methane leak rates at Aliso Canyon and subsequently at all the natural gas storage facilities in California.

These flights provided a relative comparison of the leak rates at each of the natural gas storage facilities, and are also serving as a baseline for upcoming research efforts. Researchers use a small airplane equipped to measure methane and ethane concentrations in real-time. Ethane uniquely identifies methane from a fossil fuel source, such as a natural gas reservoir, and allows the methane plume to be distinguished from other sources. By flying through the downwind methane plume at various elevations, a methane leak rate can be calculated.

Table 10 compares the average emissions rate at Aliso Canyon during the leak with the average emissions rate at all the natural gas storage facilities in California where measurements have been made. Emissions at natural gas storage facilities constitute less than 1% of statewide methane emissions. Figure 14 presents the same information in a graphical form.

Table 10: Methane Emissions at California Natural Gas Storage Facilities

Site	Date	Methane Emission (kg/hr)	Uncertainty (kg/hr)
Wild Goose	5/4/2016	ND	ND
Princeton	5/4/2016	26.9	7
Pleasant	5/4/2016	29.2	6.1
MacDonald Island	5/13/2016	277.7	60
Kirby	5/13/2016	-12.2	4
Gill Ranch	5/13/2016	10.5	8.2
Lodi	5/13/2016	-82.1	69.5
MacDonald Island	5/14/2016	247.9	48.3
Wild Goose	5/17/2016	1.1	0.6
Lodi	5/17/2016	ND	ND
Princeton	5/17/2016	41.2	6.2
Los Medanos	5/17/2016	37.3	10.7
Kirby	5/17/2016	30.7	12.5
Pleasant	5/17/2016	17.8	5.8
Macdonald	5/18/2016	478.7	85.7
Gill Ranch	5/18/2016	45.7	20.8
Los Medanos	5/20/2016	-9.7	35.1
Kirby	5/20/2016	32.3	2.7
Pleasant	5/20/2016	9.9	1.3
Los Medanos	5/22/2016	-4.4	6.3
Gill Ranch	5/22/2016	47.3	27.6
Lagoleta	5/26/2016	209	36.7
Honor Rancho	5/31/2016	413.7	112.6
Honor Rancho	6/9/2016	827.9	112.4
Macdonald	6/10/2016	315.5	67.2
Gill Ranch	6/10/2016	38.6	17.1
Macdonald	6/19/2016	534.5	155.7
Macdonald	7/6/2016	375.1	60.3

Figure 14: Methane Emissions at California Natural Gas Storage Facilities

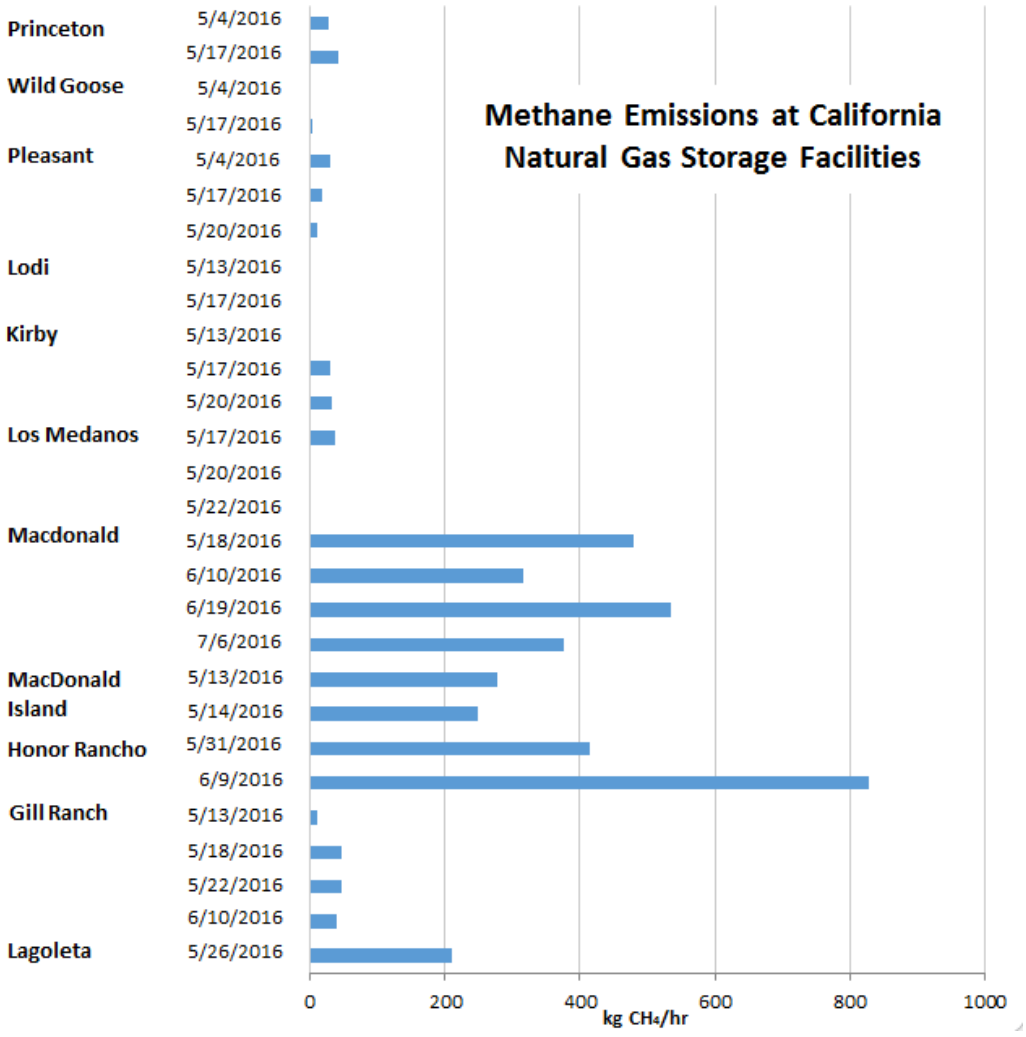

CHAPTER 6: Conclusions

Because of the urgency of the exact quantification of individual leaks that arose during this project while working on a parallel project to quantify storage facilities (PI: Fischer), and the major blowout at the Aliso Canyon facility, the focus of this project shifted more towards a better quantification of leak. That effort has resulted in great improvements in the techniques to quickly and accurately quantify surface emission sources from individual facilities (of the scale of 10-100 m). Those techniques have been demonstrated on a variety of sources and represent a major step forward for the scientific community.

While this technique is also useful for measuring the size of pipeline leaks, the research team has also learned that the ability to accurately localize a pipeline leak from the air in a single pass is realistically limited. The Princeton test showed that he research team can expect a position error of something on the order of ~200 meters (1 s) when the research team has good winds (i.e. wind speed greater than 3 ms^{-1}, constant direction). Less consistent winds require more passes to gain confidence in the leak location, leading to statistical methods of determining the location.

Fortunately, if the goal is to quantify any observed leaks, the statistics problem is dealt with through repeated passes around the source region, as the research team saw on the Princeton test. Averaging the positions of the leak locations over the multiple laps resulted in a location within 20 meters of the center of the facility.

This project demonstrated both the capabilities and limitations of in-situ gas measurements for detecting leaks from aircraft. The next step is to combine in-situ with remote sensing, e.g. one aircraft equipped with both technologies. The idea would be to fly over the pipeline at the ideal distance for the camera, and then use the in-situ measurements to quantify any leaks detected. DOE recently awarded a project to CU Boulder & UC Davis using a Frequency Comb-based Methane Observation Network in conjunction with the UCD airplane to improve the ability to detect and localize leaks at underground storage facilities. Princeton Gas has agreed to be a test site for this technology.

REFERENCES

A. Butz et al., Geophys. Res. Lett. 38, L14812 (2011).

Ackerman, K. V., and E. T. Sundquist (2008), Comparison of two US power-plant carbon dioxide emissions data sets, Environmental Science & Technology, 42(15), 5688-5693, doi:10.1021/es800221q.

Alfieri, J. G., and P. D. Blanken (2012), How representative is a point? The spatial variability of flux measurements across short distances, in *Remote Sensing and Hydrology*, edited by C. M. U. Neale and M. H. Cosh, pp. 210-214.

Bergamaschi, P., M. Krol, F. Dentener, A. Vermeulen, F. Meinhardt, R. Graul, M. Ramonet, W. Peters, and E. J. Dlugokencky (2005), Inverse modelling of national and European CH4 emissions using the atmospheric zoom model TM5, *Atmospheric Chemistry and Physics*, *5*, 2431-2460.

Beswick, K. M., T. W. Simpson, D. Fowler, T. W. Choularton, M. W. Gallagher, K. J. Hargreaves, M. A. Sutton, and A. Kaye (1998), Methane emissions on large scales, *Atmospheric Environment*, *32*(19), 3283-3291, doi:10.1016/s1352-2310(98)00080-6.

B. Miyazaki, in Underground Gas Storage: Worldwide Experiences and Future Development in the UK and Europe, D. J. Evans, R. A. Chadwick, Eds. (Geological Society, vol. 313, London, (2009), pp. 163–172

Caulton, D. R., et al. (2014), Toward a better understanding and quantification of methane emissions from shale gas development, *Proceedings of the National Academy of Sciences*, *111*(17), 6237-6242, doi:10.1073/pnas.1316546111.

Chang, R. Y. W., et al. (2014), Methane emissions from Alaska in 2012 from CARVE airborne observations, *Proceedings of the National Academy of Sciences of the United States of America*, *111*(47), 16694-16699, doi:10.1073/pnas.1412953111.

Conley, S., G. Franco, I. Faloona, D. R. Blake, J. Peischl, and T. B. Ryerson (2016), Methane emissions from the 2015 Aliso Canyon blowout in Los Angeles, CA, *Science*, *351*(6279), 1317-1320, doi:10.1126/science.aaf2348.

Conley, S. A., I. C. Faloona, D. H. Lenschow, A. Karion, and C. Sweeney (2014), A Low-Cost System for Measuring Horizontal Winds from Single-Engine Aircraft, *Journal of Atmospheric and Oceanic Technology*, *31*(6), 1312-1320, doi:10.1175/JTECH-D-13-00143.1.

Crosson, E. R. (2008), A cavity ring-down analyzer for measuring atmospheric levels of methane, carbon dioxide, and water vapor, *Applied Physics B-Lasers and Optics*, *92*(3), 403-408, doi:10.1007/s00340-008-3135-y.

Czepiel, P. M., B. Mosher, R. C. Harriss, J. H. Shorter, J. B. McManus, C. E. Kolb, E. Allwine, and B. K. Lamb (1996), Landfill methane emissions measured by enclosure and atmospheric tracer methods, *Journal of Geophysical Research-Atmospheres*, *101*(D11), 16711-16719, doi:10.1029/96jd00864.

Denmead, O. T., L. A. Harper, J. R. Freney, D. W. T. Griffith, R. Leuning, and R. R. Sharpe (1998), A mass balance method for non-intrusive measurements of surface-air trace gas exchange, *Atmospheric Environment*, *32*(21), 3679-3688, doi:10.1016/s1352-2310(98)00091-0.

Gallagher, M. W., T. W. Choularton, K. N. Bower, I. M. Stromberg, K. M. Beswick, D. Fowler, and K. J. Hargreaves (1994), MEASUREMENTS OF METHANE FLUXES ON THE LANDSCAPE SCALE FROM A WETLAND AREA IN NORTH SCOTLAND, *Atmospheric Environment*, *28*(15), 2421-2430, doi:10.1016/1352-2310(94)90394-8.

Gerbig, C., J. C. Lin, S. C. Wofsy, B. C. Daube, A. E. Andrews, B. B. Stephens, P. S. Bakwin, and C. A. Grainger (2003), Toward constraining regional-scale fluxes of CO2 with atmospheric observations over a continent: 1. Observed spatial variability from airborne platforms, *Journal of Geophysical Research-Atmospheres*, *108*(D24), doi:10.1029/2002jd003018.

Gordon, M., S. M. Li, R. Staebler, A. Darlington, K. Hayden, J. O'Brien, and M. Wolde (2015), Determining air pollutant emission rates based on mass balance using airborne measurement data over the Alberta oil sands operations, *Atmos. Meas. Tech.*, *8*(9), 3745-3765, doi:10.5194/amt-8-3745-2015.

Hacker, J. M., et al. (2016), Using airborne technology to quantify and apportion emissions of CH4 and NH3 from feedlots, *Animal Production Science*, *56*(2-3), 190-203, doi:10.1071/an15513.

Hiller, R. V., B. Neininger, D. Brunner, C. Gerbig, D. Bretscher, T. Kunzle, N. Buchmann, and W. Eugster (2014), Aircraft-based CH4 flux estimates for validation of emissions from an agriculturally dominated area in Switzerland, *Journal of Geophysical Research-Atmospheres*, *119*(8), 4874-4887, doi:10.1002/2013jd020918.

Hirsch, A. I., A. M. Michalak, L. M. Bruhwiler, W. Peters, E. J. Dlugokencky, and P. P. Tans (2006), Inverse modeling estimates of the global nitrous oxide surface flux from 1998-2001, *Global Biogeochemical Cycles*, *20*(1), doi:10.1029/2004gb002443.

J. Peischl et al., J. Geophys. Res. D Atmospheres 118, 4974–4990 (2013).

Kalthoff, N., U. Corsmeier, K. Schmidt, C. Kottmeier, F. Fiedler, M. Habram, and F. Slemr (2002), Emissions of the city of Augsburg determined using the mass balance method, *Atmospheric Environment*, *36*, S19-S31.

Karion, A., et al. (2013), Methane emissions estimate from airborne measurements over a western United States natural gas field, *Geophysical Research Letters*, *40*(16), 4393-4397, doi:10.1002/grl.50811.

K. W. Wong et al., Atmos. Chem. Phys. 15, 241–252 (2015).

Lamb, B. K., et al. (1995), DEVELOPMENT OF ATMOSPHERIC TRACER METHODS TO MEASURE METHANE EMISSIONS FROM NATURAL-GAS FACILITIES AND URBAN AREAS, *Environmental Science & Technology*, *29*(6), 1468-1479, doi:10.1021/es00006a007.

Lavoie, T. N., P. B. Shepson, M. O. L. Cambaliza, B. H. Stirm, A. Karion, C. Sweeney, T. I. Yacovitch, S. C. Herndon, X. Lan, and D. Lyon (2015), Aircraft-Based Measurements of Point Source Methane

Emissions in the Barnett Shale Basin, *Environmental Science & Technology*, *49*(13), 7904-7913, doi:10.1021/acs.est.5b00410.

Lenschow, D. H., V. Savic-Jovcic, and B. Stevens (2007), Divergence and vorticity from aircraft air motion measurements, *Journal of Atmospheric and Oceanic Technology*, *24*(12), 2062-2072, doi:10.1175/2007jtecha940.1.

Mays, K. L., P. B. Shepson, B. H. Stirm, A. Karion, C. Sweeney, and K. R. Gurney (2009), Aircraft-Based Measurements of the Carbon Footprint of Indianapolis, *Environmental Science & Technology*, *43*(20), 7816-7823, doi:10.1021/es901326b.

Miller, S. M., et al. (2013), Anthropogenic emissions of methane in the United States, *Proceedings of the National Academy of Sciences of the United States of America*, *110*(50), 20018-20022, doi:10.1073/pnas.1314392110.

M. K. McNutt et al., Proc. Natl. Acad. Sci. U.S.A. 109, 20260–20267 (2012).

Muhle, S., I. Balsam, and C. R. Cheeseman (2010), Comparison of carbon emissions associated with municipal solid waste management in Germany and the UK, *Resour. Conserv. Recycl.*, *54*(11), 793-801, doi:10.1016/j.resconrec.2009.12.009.

Neef, L., M. van Weele, and P. van Velthoven (2010), Optimal estimation of the present-day global methane budget, *Global Biogeochemical Cycles*, *24*, doi:10.1029/2009gb003661.

Nisbet, E., and R. Weiss (2010), Top-Down Versus Bottom-Up, *Science*, *328*(5983), 1241-1243, doi:10.1126/science.1189936.

Peischl, J., et al. (2010), A top-down analysis of emissions from selected Texas power plants during TexAQS 2000 and 2006, *Journal of Geophysical Research-Atmospheres*, *115*, 15, doi:10.1029/2009jd013527.

Peischl, J., et al. (2013), Quantifying sources of methane using light alkanes in the Los Angeles basin, California, *Journal of Geophysical Research-Atmospheres*, *118*(10), 4974-4990, doi:10.1002/jgrd.50413.

Petron, G., et al. (2014), A new look at methane and nonmethane hydrocarbon emissions from oil and natural gas operations in the Colorado Denver-Julesburg Basin, *Journal of Geophysical Research-Atmospheres*, *119*(11), 6836-6852, doi:10.1002/2013jd021272.

Quick, J. C. (2014), Carbon dioxide emission tallies for 210 U.S. coal-fired power plants: A comparison of two accounting methods, *J. Air Waste Manage. Assoc.*, *64*(1), 73-79, doi:10.1080/10962247.2013.833146.

R. A.Washenfelder, P. O.Wennberg, G. C. Toon, Geophys. Res. Lett. 30, 2226 (2003).

Ritter, J. A., J. D. W. Barrick, C. E. Watson, G. W. Sachse, G. L. Gregory, B. E. Anderson, M. A. Woerner, and J. E. Collins (1994), AIRBORNE BOUNDARY-LAYER FLUX MEASUREMENTS OF TRACE SPECIES OVER CANADIAN BOREAL FOREST AND NORTHERN WETLAND REGIONS, *Journal of Geophysical Research-Atmospheres*, *99*(D1), 1671-1685, doi:10.1029/93jd01859.

R. O. Green et al., Remote Sens. Environ. 65, 227–248 (1998).

Roscioli, J. R., et al. (2015), Measurements of methane emissions from natural gas gathering facilities and processing plants: measurement methods, *Atmos. Meas. Tech.*, *8*(5), 2017-2035, doi:10.5194/amt-8-2017-2015.

Ryerson, T. B., et al. (1998), Emissions lifetimes and ozone formation in power plant plumes, *Journal of Geophysical Research-Atmospheres*, *103*(D17), 22569-22583, doi:10.1029/98jd01620.

South Coast Air Quality Management District, "Laboratory results" (2016); srvwww.aqmd.gov/home/regulations/compliance/aliso-canyon-update/gas-sample-near-leakingwell/laboratory-results [accessed 13 February 2016].

T. B. Ryerson et al., Proc. Natl. Acad. Sci. U.S.A. 109, 20246–20253 (2012).

Tratt, D. M., K. N. Buckland, J. L. Hall, P. D. Johnson, E. R. Keim, I. Leifer, K. Westberg, and S. J. Young (2014), Airborne visualization and quantification of discrete methane sources in the environment, *Remote Sensing of Environment*, *154*, 74-88, doi:10.1016/j.rse.2014.08.011.

Turnbull, J. C., et al. (2011), Assessment of fossil fuel carbon dioxide and other anthropogenic trace gas emissions from airborne measurements over Sacramento, California in spring 2009, *Atmospheric Chemistry and Physics*, *11*(2), 705-721, doi:10.5194/acp-11-705-2011.

U.S. Environmental Protection Agency (EPA), "Benzene" (2014); http://cfpub.epa.gov/ncea/iris2/chemicalLanding.cfm?substance_nmbr=276.

Wecht, K. J., D. J. Jacob, C. Frankenberg, Z. Jiang, and D. R. Blake (2014), Mapping of North American methane emissions with high spatial resolution by inversion of SCIAMACHY satellite data, *Journal of Geophysical Research-Atmospheres*, *119*(12), 7741-7756, doi:10.1002/2014jd021551.

Willis, G. E., and J. W. Deardorff (1976), LABORATORY MODEL OF DIFFUSION INTO CONVECTIVE PLANETARY BOUNDARY-LAYER, *Quarterly Journal of the Royal Meteorological Society*, *102*(432), 427-445, doi:10.1002/qj.49710243212.

Wratt, D. S., N. R. Gimson, G. W. Brailsford, K. R. Lassey, A. M. Bromley, and M. J. Bell (2001), Estimating regional methane emissions from agriculture using aircraft measurements of concentration profiles, *Atmospheric Environment*, *35*(3), 497-508, doi:10.1016/s1352-2310(00)00336-8.

Yacovitch, T. I., et al. (2014), Demonstration of an Ethane Spectrometer for Methane Source Identification, *Environmental Science & Technology*, *48*(14), 8028-8034, doi:10.1021/es501475q.

Yuan, B., et al. (2015), Airborne flux measurements of methane and volatile organic compounds over the Haynesville and Marcellus shale gas production regions, *Journal of Geophysical Research-Atmospheres*, *120*(12), 6271-6289, doi:10.1002/2015jd023242.

APPENDIX A

Methane Emissions at Different Facilities in California

Site	Date	Methane Emission (kg/hr)	Uncertainty (kg/hr)
Wheeler Compressor (Socal Gas)	9/2/2016	79.5	23.8
PG&E Compressor station - Kettleman	9/2/2016	1.7	8.8
SDG&E – Moreno Station	9/3/2016	38.4	7.9
SCG – Blythe Compressor	9/3/2016	133.7	52.6
SCG – South Needles Station	9/3/2016	10.2	3.1
Wild Goose (compressor)	9/11/2016	143.4	38
Panoche Energy Compressor	9/13/2016	140	15.7
Crows Landing Landfill	9/13/2016	94.4	23.8
Oak Flat Road Gas (37.422N,121.150W)	9/13/2016	18.4	47.6
Tracey Biomass Plant	9/13/2016	136.4	27.3
Honor Rancho Storage	9/15/2016	60.6	204.8
Newberry Compressor	9/15/2016	66.9	14.9
Burney Compessor	9/10/2016	86.7	17.6

Methane Emissions at California Natural Gas Storage Facilities (full table)

Date	Methane Emission (kg/hr)	Uncertainty (kg/hr)	Ethane emission (kg/hr)	Uncertainty (kg/hr)2	Laps	Wind Direction	Wind Speed (m/s)	Flux Ratio Eth/Meth	Fit	Uncertainty	Start UTC s-midnight	End UTC s-midnight	Lowest Altitude	Highest Altitude	Surface Fraction
5/4/16	ND	ND	ND	ND	7	21	7.1	0.00	0.005	0.000	62973	63356	77	211	0.12
5/4/16	26.9	7	1.6	0.7	12	12	8.4	0.03	0.01	0.001	63669	64871	93	250	0.57
5/4/16	29.2	6.1	1.1	0.3	20	27	4.2	0.02	0.01	0.001	66196	67735	64	314	0.36
5/13/16	277.7	60	21.2	6.3	21	281	7.0	0.04	0.02	0.001	72368	74644	86	399	0.48
5/13/16	-12.2	4	-1.8	0.9	7	245	12.4	0.08	0.06	0.004	75410	76462	71	262	0.22
5/13/16	10.5	8.2	1.5	0.5	26	328	6.3	0.08	0.01	0.001	79648	81063	42	365	0.71
5/13/16	-82.1	69.5	-16.4	5.8	12	267	7.6	0.11	0.03	0.002	83577	84973	89	446	-0.32
5/14/16	247.9	48.3	20.5	5	25	294	6.1	0.04	0.03	0.002	68720	71694	83	573	0.27
5/17/16	1.1	0.6	0.2	0	7	338	9.2	0.12	0.00	0.001	70559	71065	98	259	-0.6
5/17/16	ND	ND	ND	ND	ND										
5/17/16	41.2	6.2	2.4	0.8	13	341	10.1	0.03	0.01	0.001	71311	72500	66	219	0.6
5/17/26	37.3	10.7	2.3	0.8	10	355	5.9	0.03	0.03	0.002	78485	80207	99	438	0.2
5/17/16	30.7	12.5	2.6	1.9	16	1	8.9	0.05	0.03	0.002	75608	78056	40	289	0.38
5/17/16	17.8	5.8	1	0.4	11	4	8.9	0.03	0.02	0.001	73730	74895	49	207	0.41
5/18/16	478.7	85.7	39.2	8.9	47	335	4.8	0.044	0.027	0.0016	65190	70593	82	810	0.2
5/18/16	45.7	20.8	3.6	0.9	16	307	5.3	0.042	0.013	0.0008	72992	75404	43	459	0.02
5/20/16	-9.7	35.1	-0.2	4.7	15	258	9	0.013	0.031	0.0019	64624	67385	156	410	-1.72
5/20/16	32.3	2.7	1.8	0.3	13	251	9.1	0.029	0.020	0.0013	62447	64245	46	229	0.16
5/20/16	9.9	1.3	0.7	0.2	14	259	5	0.036	0.019	0.0013	60186	61678	45	228	0.26

Date	Methane Emission (kg/hr)	Uncertainty (kg/hr)	Ethane emission (kg/hr)	Uncertainty (kg/hr)2	Laps	Wind Direction	Wind Speed (m/s)	Flux Ratio Eth/Meth	Fit	Uncertainty	Start UTC s-midnight	End UTC s-midnight	Lowest Altitude	Highest Altitude	Surface Fraction
5/22/16	-4.4	6.3	-1.1	2.5	11	259	6.1	0.132	0.034	0.0021	62916	65125	187	325	1.43
5/22/16	47.3	27.6	2.8	0.7	40	286	2.5	0.031	0.007	0.0004	72307	78776	33	1291	-0.06
5/26/16	209	36.7	9.6	2.9	17	228	2.9	0.025	0.023	0.0014	72579	76481	159	466	0.44
5/31/16	413.7	112.6	11.8	2.2	20	225	4.7	0.015	0.005	0.0003	81880	85137	141	786	-0.02
6/9/16	827.9	112.4			23	223	5.2				80844	85107	143	733	0.42
6/10/16	315.5	67.2	15.9	2.5	11	285	8.1	0.027	0.007	0.0005	84778	85995	119	431	0.24
6/10/16	38.6	17.1	4.2	0.8	19	334	4.6	0.059	0.001	0.0006	77896	80682	54	328	0.67
6/19/16	534.5	155.7	42.7	11.7	32	317	3.1	0.043	0.025	0.0015	76758	81081	105	1076	0.22
7/6/2016	375.1	60.3	28.4	5.6	26	281	6.4	0.038	0.0319	0.002	83515	86830	90	465	0.23